coatings

MDPI

Communication

Cleaning Effect of Atmospheric-Plasma-Sprayed Y_2O_3 Coating Using Piranha Solution Based on Contamination Particle Measurement

Hyuksung Kwon [1,2], Minjoong Kim [2,3], Jongho So [2,3], Seonjeong Maeng [2], Jae-Soo Shin [1] and Ju-Young Yun [2,4,*]

[1] Department of Advanced Materials Engineering, Daejeon University, Daejeon 34520, Republic of Korea
[2] Vacuum Materials Measurement Team, Korea Research Institute of Standards and Science, Daejeon 34113, Republic of Korea
[3] Department of Electrical Engineering, Hanyang University, Seoul 04763, Republic of Korea
[4] Division of Nanoscience and Technology, University of Science and Technology, Daejeon 34113, Republic of Korea
* Correspondence: jyun@kriss.re.kr; Tel.: +82-42-868-5669

Abstract: A Y_2O_3 coating was prepared using the atmospheric plasma spraying (APS) technique. On exposing the coating to $CF_4/O_2/Ar$ plasma, a fluorine contamination layer (YO_xF_y) was formed, which was the main cause of process drift and contamination particle generation on the APS–Y_2O_3 coating surface. To remove the YO_xF_y layer on the coating surface, a piranha solution, which is a mixture of sulfuric acid and hydrogen peroxide, was employed for cleaning. The piranha solution was found to be an excellent medium for removing the YO_xF_y layer. The amount of contamination particle generated could be reduced by approximately 37% after cleaning with a 3:1 piranha solution compared with before cleaning.

Keywords: yttrium oxide (Y_2O_3); atmospheric plasma spraying (APS); cleaning process; contamination particle; plasma etching

Citation: Kwon, H.; Kim, M.; So, J.; Maeng, S.; Shin, J.-S.; Yun, J.-Y. Cleaning Effect of Atmospheric-Plasma-Sprayed Y_2O_3 Coating Using Piranha Solution Based on Contamination Particle Measurement. *Coatings* **2023**, *13*, 653. https://doi.org/10.3390/coatings13030653

Received: 11 January 2023
Revised: 21 February 2023
Accepted: 16 March 2023
Published: 20 March 2023

1. Introduction

Plasma is used in various processes, such as etching, deposition, and cleaning, in the semiconductor/display industry. Since the etching process uses plasma composed of highly reactive carbon-, fluorine-, and chlorine-based compounds, it induces a chemical reaction with the internal components of the chamber. The by-products of this reaction formed on the surface are deposited on the surrounding parts, generating contamination particles, which ultimately affect the product yield [1–5]. Therefore, the chamber wall and internal parts are coated with plasma-resistant materials using various coating methods for the semiconductor etching process. Al_2O_3 and Y_2O_3 are widely used as ceramic coating materials exhibiting plasma corrosion resistance [6–15]. Conventionally, Al_2O_3 has been used as a representative plasma corrosion resistance material owing to its low price and easy sintering process. However, it lacks chemical stability to highly reactive halogen element radicals. Y_2O_3 is widely applied as a plasma corrosion resistance material owing to its lower etch rate and better chemical stability than Al_2O_3 for fluorine-based plasma during the semiconductor etching process. The atmospheric plasma spraying (APS) coating method is commonly used in the industry; this is attributed to the fewer restrictions on raw materials and coating conditions, ease of control of the coating thickness, realization of complex shapes, and coating application over a large area [14–16]. However, when an atmospheric-plasma-sprayed Y_2O_3 coating is exposed to highly reactive fluorine-based plasma for a long duration, there is surface corrosion, and a YO_xF_y layer, which is a fluorinated layer, is formed. The YO_xF_y layer is the main cause of process drift and contamination particle generation [8,10]. To remove the fluorine contamination layer after plasma exposure, efforts

have been made to clean and reuse the coating surface [17,18]. Cleaning a plasma-resistant coating requires physically etching the surface using a surfactant, and the degree of cleaning should be evaluated again after visual observation. Despite this problem, there has been no technical research on the cleaning technology for plasma-resistant coatings.

In this study, a piranha solution was used for cleaning a APS-Y_2O_3 coating for the first time. A piranha solution is a mixture of sulfuric acid and hydrogen peroxide; it is a very strong oxidizing agent and has highly corrosive properties. It is used to remove organic residues and to dissolve metal oxides and carbonates [19–22]. We applied it to the cleaning of a plasma corrosion resistance coating owing to its potential for dissolving the fluorine contamination layer on the APS–Y_2O_3 coating surface. Currently, most studies on the use of the piranha solution have been conducted focusing on Si wafer cleaning, and research on the cleaning of plasma corrosion resistance coating, which is important in the semiconductor industry, is lacking. In this work, a APS–Y_2O_3 coating exposed to $CF_4/O_2/Ar$ plasma was cleaned using piranha solutions prepared at different ratios (2:1, 3:1, 4:1, and 5:1). Before and after the cleaning process, the formation of a residual fluorine contamination layer on the APS–Y_2O_3 coating was confirmed, and the amount of contamination particle generated was analyzed and compared.

2. Experimental

We prepared an aluminum 6061-T6 alloy (HIGGLAB, Seoul, Republic of Korea) in the form of a circular sample with dimensions of 76.2 ø × 3 mm. The substrates were coated by APS (Axial III, Northwest Mettech, Surrey, BC, Canada), where Y_2O_3 was in a powder form (99.99%, 25–30 μm, Tokyo, Japan, Figure 1). The APS coating was applied with Ar sprayed as a carrier gas at 1500 Torr, and the plasma gun power was set to 980 W.

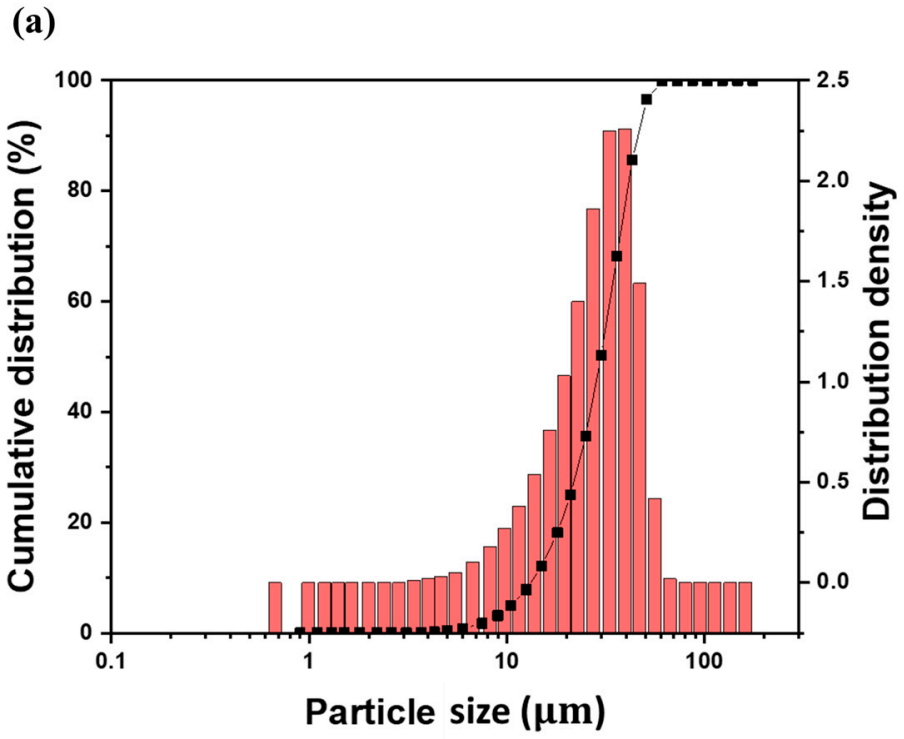

Figure 1. *Cont.*

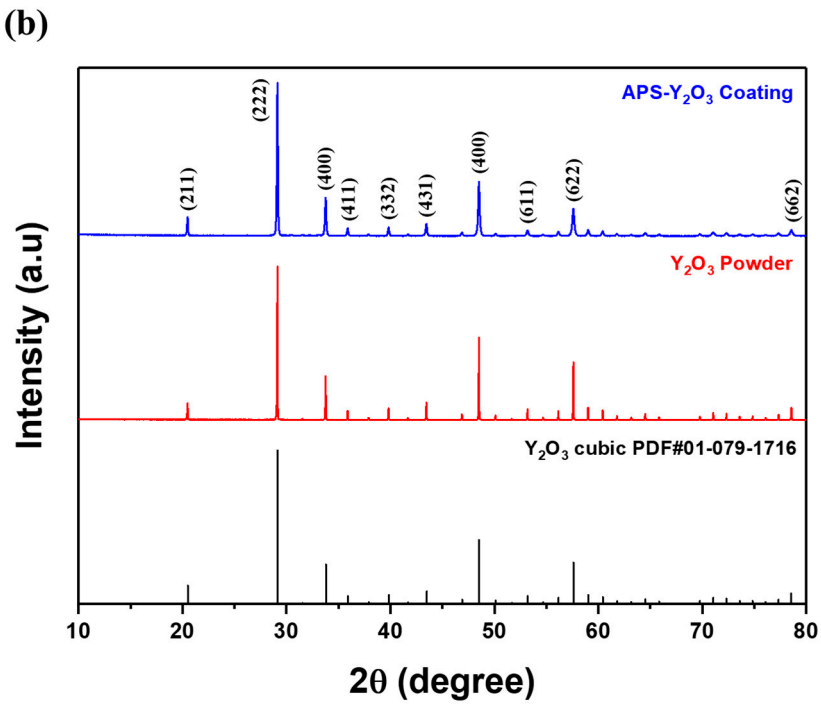

Figure 1. (**a**) Powder size analysis of the Y_2O_3 coating, (**b**) XRD patterns of Y_2O_3 powder and APS–Y_2O_3 coating.

To evaluate the plasma resistance of the APS–Y_2O_3 coating, a vertical conductively coupled plasma-reactive ion etching (VCCP-RIE) system was used, as shown in Figure 2. The plasma density was enhanced by arranging a niobium magnet in 1000 G on the upper electrode. The RF power used was 13.56 MHz (Sizer Generator, Advanced Energy, Fort Collins, CO, USA), and an impedance matching network was employed (Navigator, Advanced Energy, Fort Collins, Denver, CO, USA). It was exposed to fluorine-based plasma ($CF_4/O_2/Ar$) used in the etching process; Table 1 presents the detailed conditions. The contamination particles generated due to plasma exposure were measured in real time using an in situ particle monitor (ISPM; Stiletto, INFICON, Heidland, Switzerland). To compare the amount of contamination particle generated before and after cleaning with the piranha solution, the APS–Y_2O_3 coating was first exposed to $CF_4/O_2/Ar$ plasma. Subsequently, the amount of contamination particle generated by re-exposure to the $CF_4/O_2/Ar$ plasma without any cleaning was compared with the amount of contamination particle generated after the cleaning.

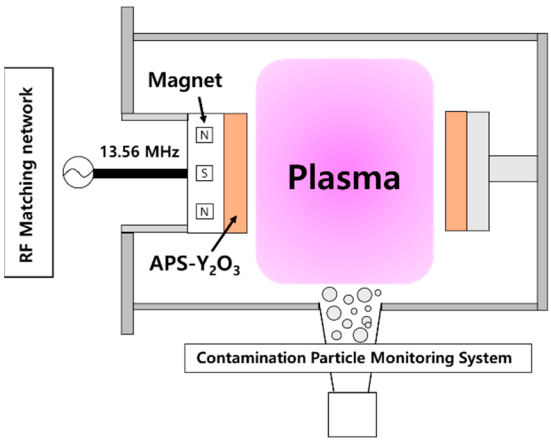

Figure 2. Schematic of a vertical conductively coupled plasma etching system.

Table 1. Details of the plasma etching parameters.

Plasma Etching Parameters	
Gas	$CF_4/O_2/Ar$ 20, 5, 15 sccm
Working pressure	250–262 mTorr
Power	200 W
Etch time	60 min

The piranha solution was prepared in different volume ratios by mixing sulfuric acid (extra pure grade 95%, DUKSAN, Seoul, Republic of Korea) and hydrogen peroxide (extra pure grade 30%, DUKSAN, Seoul, Republic of Korea). Table 2 presents the preparation conditions of the piranha solutions. The piranha solution was maintained at a temperature of 70 °C using a heating stage (Hotplates & Stirrer, MTOPS, Seoul, Republic of Korea). Figure 2 shows the schematic of a vertical conductively coupled plasma etching system. First, the APS–Y_2O_3 coating was exposed to $CF_4/O_2/Ar$ plasma, and later dipped in a piranha solution for 5 min. After rinsing in DI water, it was cleaned 100 times using a #800 grit scouring pad. Figure 3 shows the experimental method of piranha solution cleaning. The morphologies of the APS–Y_2O_3 coating surface before and after cleaning with the piranha solution were analyzed by field emission scanning electron microscopy (FE-SEM, Secondary electron, S-4800, Hitachi, Tokyo, Japan). APS-Y_2O_3 coating was coated by Pt using the sputtering method. The residual components on the APS–Y_2O_3 coating surface were analyzed by X-ray photoelectron spectroscopy (XPS, Al Kα 1486.6 eV, 45° from sample surface, PHU 5000 VersaProbe, Ulvac-PHI, Hagisono, Japan). The surface roughness was analyzed by confocal microscopy.

Table 2. Details of the piranha solution ratio.

Piranha Solution Ratio		
$H_2SO_4 + H_2O_2$	2:1	40 mL, 20 mL
	3:1	45 mL, 15 mL
	4:1	48 mL, 12 mL
	5:1	50 mL, 10 mL

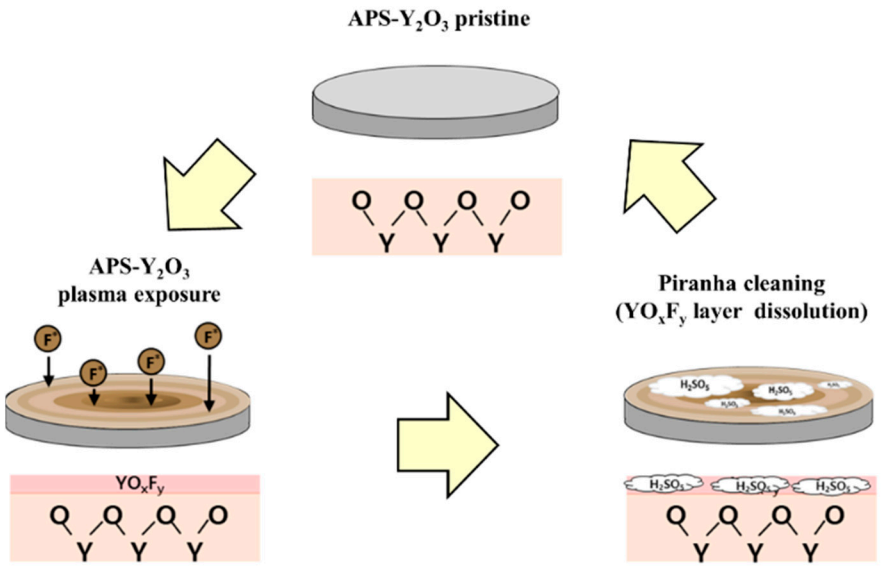

Figure 3. Schematic of cleaning experiments conducted to remove the fluorination layer on the APS–Y_2O_3 coating surface.

3. Results

Figure 4 shows the surface images of the APS–Y_2O_3 coating before and after $CF_4/O_2/Ar$ plasma exposure and after cleaning with the piranha solution. Figure 4a shows the surface image of pristine APS–Y_2O_3 before plasma exposure, and Figure 4b shows the image after plasma exposure. After exposure to fluorine-based plasma, a brown contamination pattern was formed on the coating surface. This is a fluorine contamination layer due to surface fluorination, which generates contamination particles [17,18]. Figure 4c–f shows that the APS–Y_2O_3 coating surface exposed to plasma was cleaned with piranha solutions prepared at ratios of 2:1, 3:1, 4:1, and 5:1, respectively. The fluorine contamination layer was removed regardless of the piranha solution ratio. Figure 5 shows the FE-SEM image for a more detailed surface analysis.

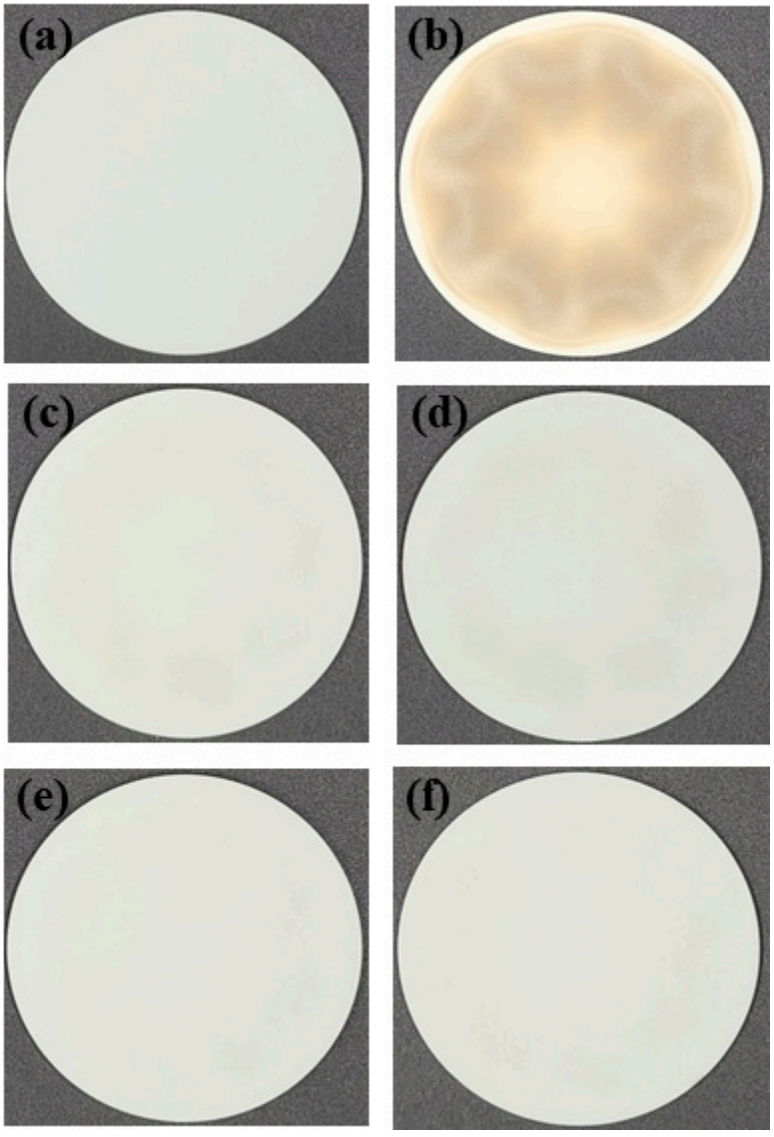

Figure 4. Surface images of APS–Y_2O_3 coating specimens: (**a**) pristine APS–Y_2O_3, (**b**) APS–Y_2O_3 plasma exposure, and after cleaning with piranha solutions prepared at ratios of (**c**) 2:1, (**d**) 3:1, (**e**) 4:1, and (**f**) 5:1.

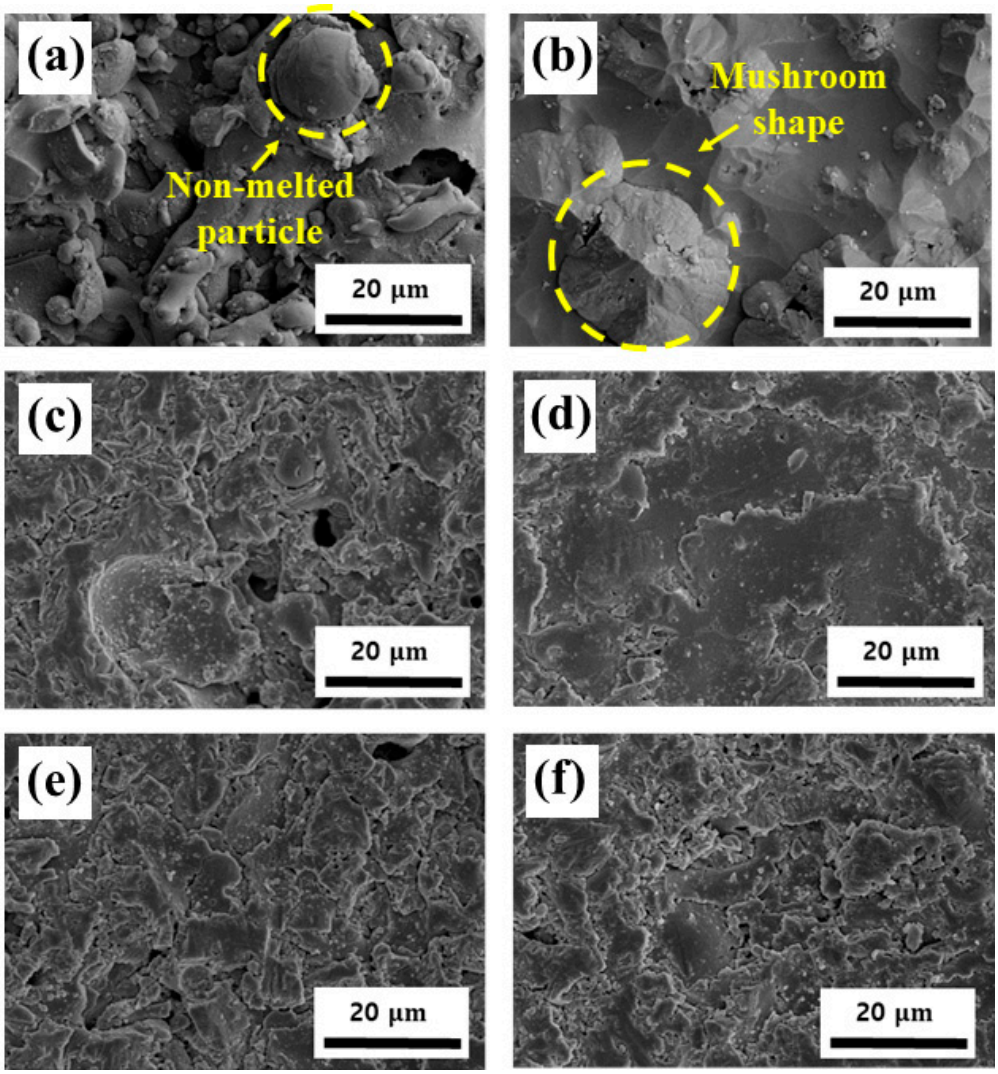

Figure 5. FE-SEM images of the surface of APS–Y_2O_3 coatings; (**a**) pristine APS–Y_2O_3, (**b**) APS–Y_2O_3 plasma exposure and after cleaning with piranha solutions with ratios of (**c**) 2:1, (**d**) 3:1, (**e**) 4:1, and (**f**) 5:1.

Figure 5a,b show the surface images before and after plasma exposure of the APS–Y_2O_3 coating, respectively. In Figure 5a, pores and nonmelted particles can be observed, which is common on an APS coating surface [15]. The APS coating powder has a size range of 30–50 μm, which is greater than those of other spray coatings [8,12]. In addition, the droplets were rapidly cooled as they collided with the substrate. Because of this, nonmelted particles were formed. Plasma erosion occurs from the edge of the nonmelted particles. Consequently, a mushroom-shaped etching trace could be observed, as shown in Figure 5b. Figure 5c–f shows the surface images after cleaning with piranha solutions prepared at ratios of 2:1, 3:1, 4:1, and 5:1, respectively. After cleaning with piranha solutions with ratios of 2:1, 4:1, and 5:1, a relatively rough surface with some pores was observed. In contrast, after cleaning with a piranha solution at a ratio of 3:1, a smooth surface with the least number of defects was observed.

Figure 6 shows the EDS mapping image, where the presence of a fluorine contamination layer on the APS–Y_2O_3 coating surface can be confirmed. The pristine APS–Y_2O_3 coating surface did not contain any fluorine, as shown in Figure 6a. Conversely, the APS–Y_2O_3 coating exposed to $CF_4/O_2/Ar$ plasma showed a high fluorine content on the surface, as shown in Figure 6b. From this, it can be confirmed that the surface of the APS–Y_2O_3 coating was fluorinated by plasma. Figure 6c–f shows the APS–Y_2O_3 coating

after cleaning with piranha solutions with ratios of 2:1, 3:1, 4:1, and 5:1, respectively. Regardless of the piranha solution ratio, the surface fluorine content decreased under all the conditions.

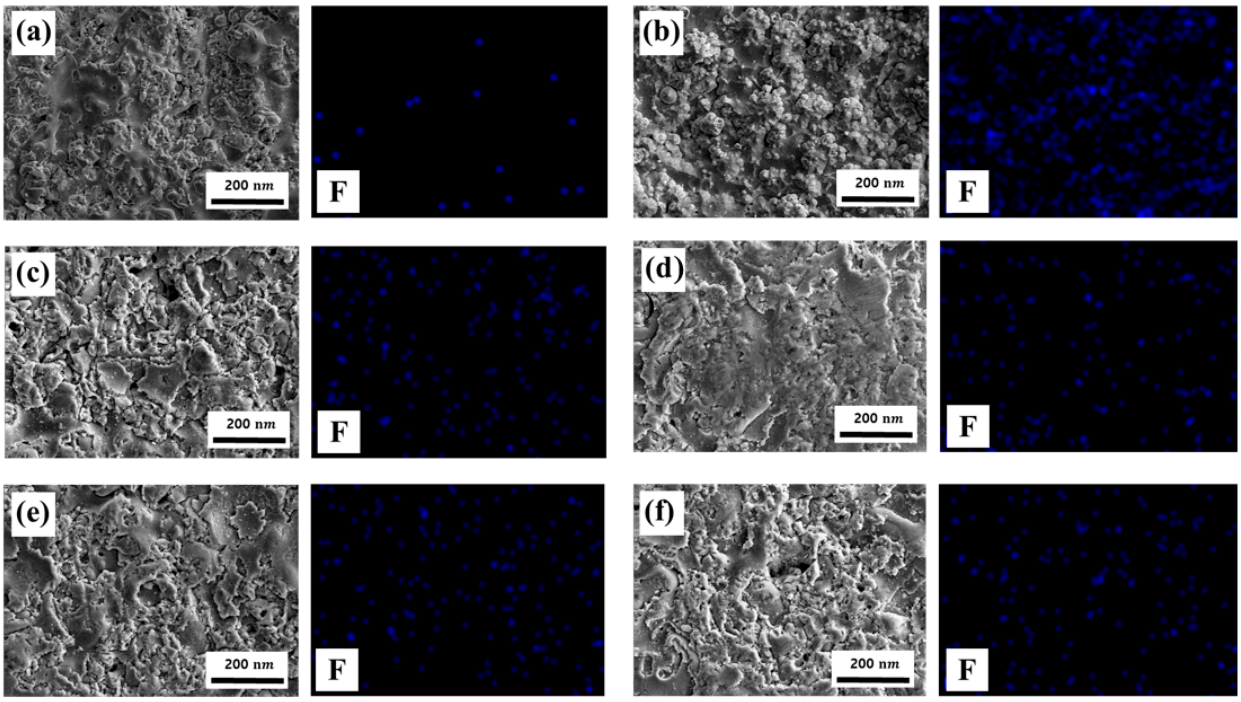

Figure 6. EDS mapping (fluorine "F") images of the surface of APS–Y_2O_3 coatings: (**a**) pristine APS–Y_2O_3, (**b**) APS–Y_2O_3 plasma exposure and after cleaning with piranha solutions prepared at ratios of (**c**) 2:1, (**d**) 3:1, (**e**) 4:1, and (**f**) 5:1.

Figure 7 shows the XPS spectra and Ar ion sputtering depth profile of the APS–Y_2O_3 coating surface before and after $CF_4/O_2/Ar$ plasma exposure and after piranha cleaning. Figure 7a shows an image of the APS–Y_2O_3 coating before plasma exposure. This process was performed in an atmospheric environment; therefore, the carbon present in the air penetrated the coating surface and existed therein. Therefore, carbonate bonding can be observed in Figure 7a. In the pristine APS–Y_2O_3 coating, the Y $3d_{3/2}$ and Y $3d_{5/2}$ peak positions were 157.6 and 155.5 eV, and two peaks had a difference of 2.1 eV with an intensity ratio of 3:2 in their binding energy [23,24]. After $CF_4/O_2/Ar$ plasma exposure, the fluorine present on the surface was approximately 35%, and the Y–O bonds were replaced by Y–F bonds owing to surface fluorination. The Y–O and Y–F binding energies of Y $3d_{3/2}$ were 161.2 and 159.0 eV and those of Y $3d_{5/2}$ increased to 159.1 and 156.9 eV, respectively. This can be possibly attributed to the higher electronegativity of fluorine (4.0) atoms than oxygen (3.5) atoms [9,16]. Figure 7c–f shows XPS spectra and Ar ion sputtering depth profile, after cleaning with the piranha solution. The coating surface depth profile analysis shows that, after cleaning with the piranha solutions with ratios of 2:1, 3:1, 4:1, and 5:1, the fluorine content on the coating surface decreased to 2.49%, 2.35%, 3.18%, and 4.17%, respectively, decreasing within 5% regardless of the piranha solution ratio. Moreover, the binding energies of the Y $3d_{3/2}$ and Y $3d_{5/2}$ peaks were 158.0 and 155.9 eV, respectively. The binding energy was similar to that of the pristine APS–Y_2O_3 coating.

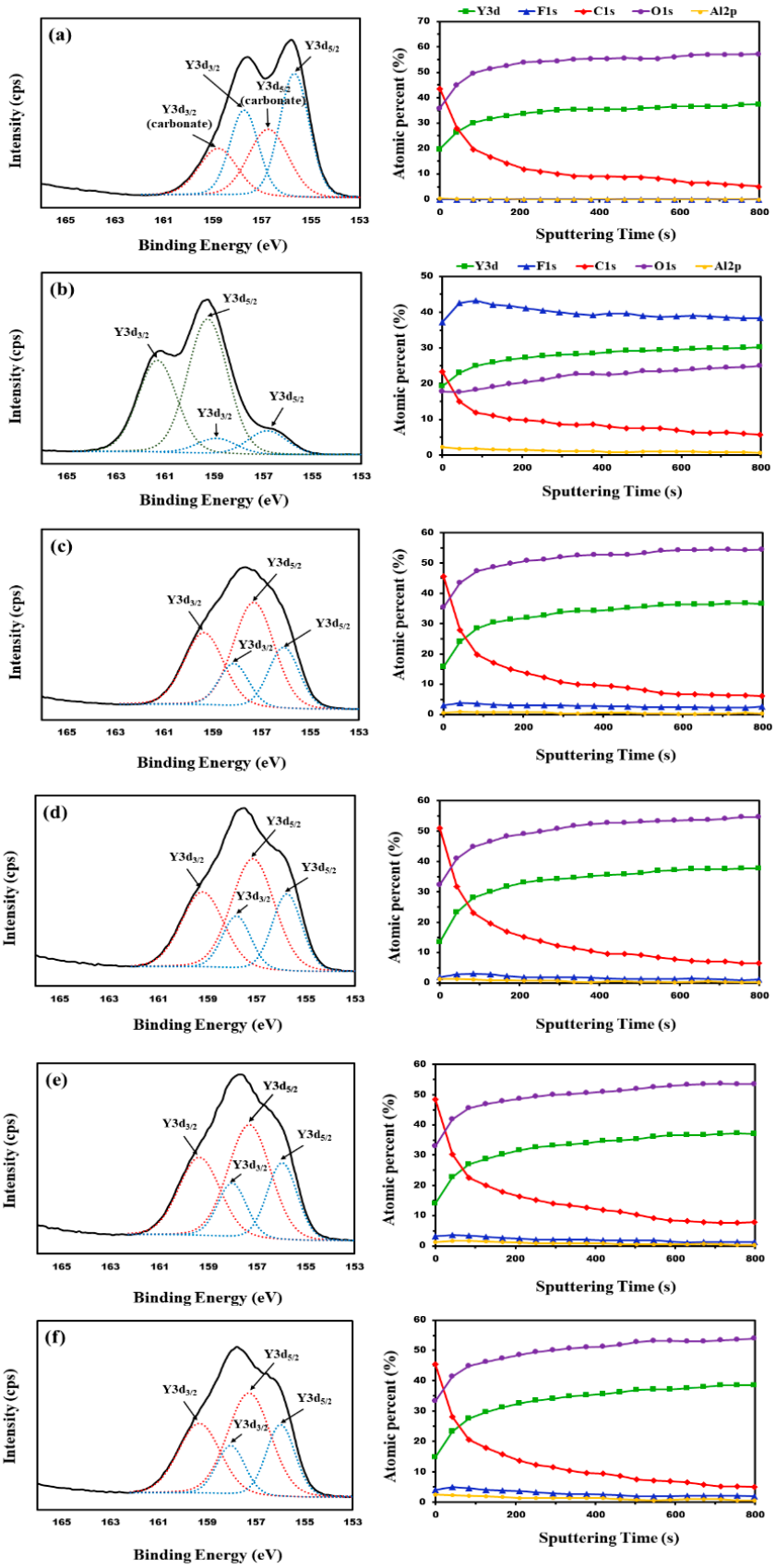

Figure 7. XPS spectrum of the surface of APS–Y_2O_3 coatings and Ar ion sputtering depth profile: (**a**) pristine APS–Y_2O_3, (**b**) APS–Y_2O_3 plasma exposure and after cleaning with piranha solutions prepared at ratios of (**c**) 2:1, (**d**) 3:1, (**e**) 4:1, and (**f**) 5:1.

Figure 8 shows the surface roughness of the APS–Y_2O_3 coating before and after plasma exposure and after cleaning with the piranha solution. The pristine APS–Y_2O_3 coating shows a rough surface (Ra = 0.716 µm) in Figure 8a. The APS coating uses a large powder size of approximately 30 µm. It is melted by the plasma jet and hits the substrate. At the same time, it cools rapidly, and nonmelted particles and pores are formed. Figure 8b shows the surface roughness of the APS–Y_2O_3 coating exposed to the $CF_4/O_2/Ar$ plasma; the surface roughness value is lower than that of the pristine APS–Y_2O_3 coating. This was caused by flattening under continuous Ar^+ bombardment. Figure 8c–f shows the surface roughness after cleaning with the piranha cleaning. At a ratio of 2:1, the roughness was similar to that of the pristine APS–Y_2O_3 coating. In particular, at a ratio of 3:1, the surface was relatively smooth, consistent with the SEM image shown in Figure 6. The surface roughness values under the other conditions were Ra = 0.582 and 0.654 µm, respectively, reflecting a smoother surface than the pristine APS–Y_2O_3 coating. These results confirmed that cleaning with the 3:1 piranha solution helped remove the most amount of fluorine contamination layer on the APS–Y_2O_3 coating, while imparting the smoothest surface.

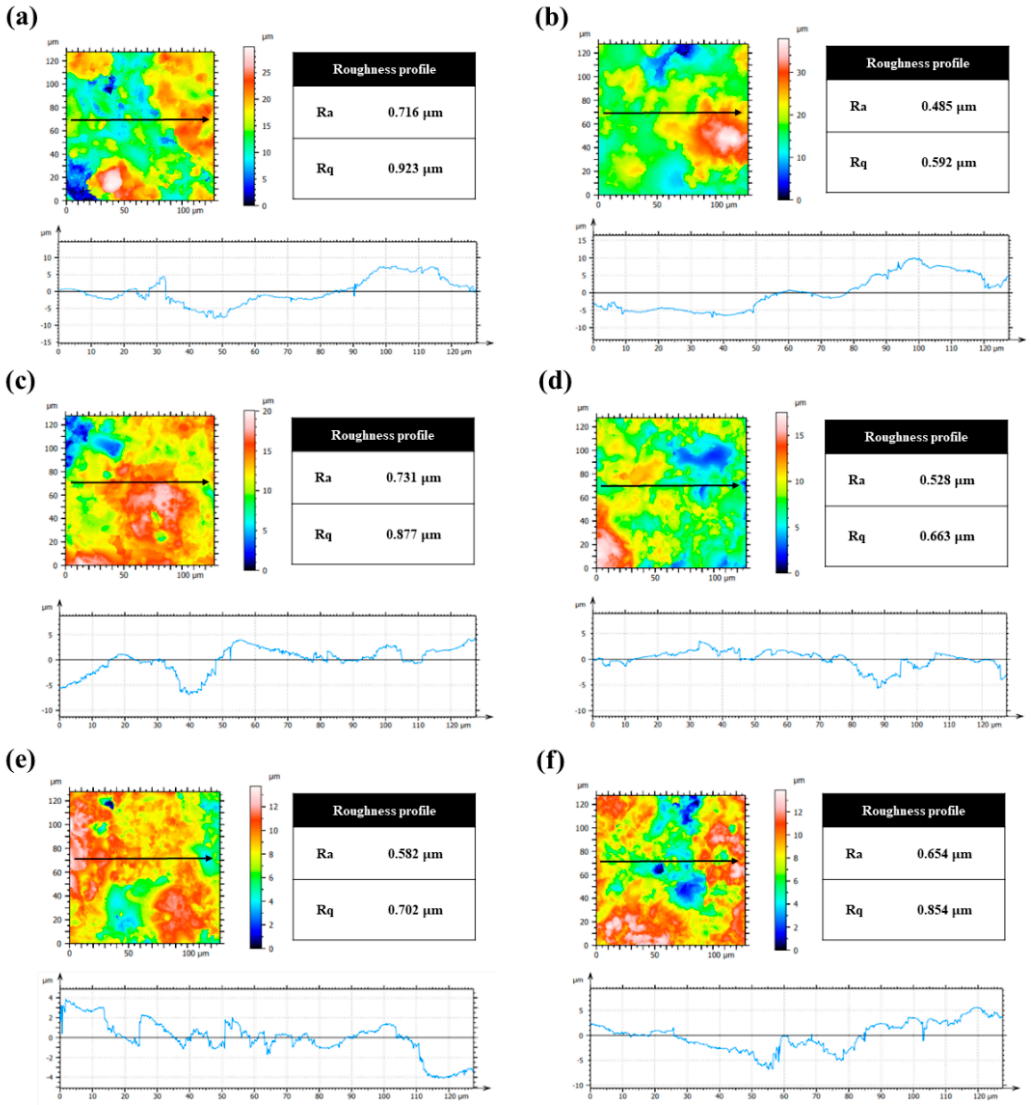

Figure 8. Confocal microscopy surface roughness of the APS–Y_2O_3 coating: (**a**) pristine APS–Y_2O_3, (**b**) APS–Y_2O_3 plasma exposure and after cleaning with piranha solutions prepared at ratios of (**c**) 2:1, (**d**) 3:1, (**e**) 4:1, and (**f**) 5:1.

Figure 9 shows the amount of contamination particles generated when the APS–Y_2O_3 coating was exposed to $CF_4/O_2/Ar$ plasma. In Figure 9a, the amount of contamination particles generation in the APS–Y_2O_3 pristine coating is 450 EA. When re-exposed to plasma without cleaning, this amount increased by approximately twofold to 867 EA, as shown in Figure 9b. This increase can be attributed to the surface corrosion caused by the plasma. On the other hand, the amounts of contamination particle generated after cleaning with piranha solutions at ratios of 2:1, 3:1, 4:1, and 5:1 were 857, 542, 663, and 757 EA, respectively. At a ratio of 3:1, the amount of contamination particle generation reduced by approximately 37% compared to that without cleaning; this is because the surface of the APS–Y_2O_3 coating had fewer surface defects and a denser microstructure, such as a smooth surface, compared to that observed for ratios of 2:1, 4:1, and 5:1, and the XPS analysis showed that the surface had the lowest fluorine content (2.35%). The fluorine contamination layer formed on the APS–Y_2O_3 coating surface was removed to the maximum extent, and the amount of contamination particles generated was the least.

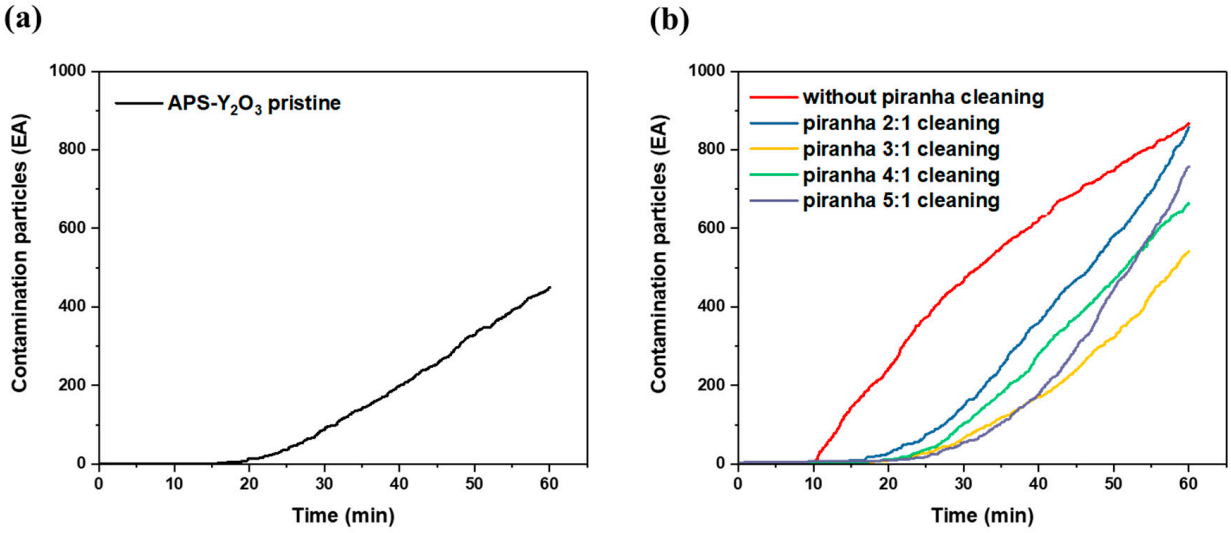

Figure 9. Real-time detection of contamination particles generated from the APS–Y_2O_3 coating: (**a**) pristine APS–Y_2O_3, (**b**) with and without cleaning with the piranha solution.

4. Conclusions

We exposed an APS–Y_2O_3 coating to $CF_4/O_2/Ar$ plasma and confirmed the formation of a fluorine contamination layer on the coating surface, which was the cause of contamination particle generation. Subsequently, the APS–Y_2O_3 coating was cleaned using piranha solutions prepared at ratios of 2:1, 3:1, 4:1, and 5:1, and the change in the coating surface properties and the amount of contamination particle generated after cleaning were investigated. Regardless of the piranha ratio, the fluorine contamination layer formed on the coating surface could be reduced to approximately 5%. In particular, after cleaning with a 3:1 piranha solution, the surface fluorine content was the lowest, and the surface was the smoothest. The amount of contamination particle generated from the pristine APS–Y_2O_3 coating was 450 EA, and when re-exposed to plasma without any cleaning, this amount increased by two folds to 867 EA compared with that of the pristine APS–Y_2O_3 coating. This increase is attributed to the corrosion caused by the plasma. Cleaning with the piranha solution reduced the amount of contamination particle generated compared to before cleaning. For a ratio of 3:1, the contamination particle generated reduced by approximately 37% compared with that before cleaning, and it was most similar to the pristine APS–Y_2O_3 coating. Therefore, we confirmed that cleaning with the 3:1 piranha solution produced a coating property similar to that of the pristine APS–Y_2O_3 coating.

Author Contributions: Conceptualization, H.K. and M.K.; methodology, H.K. and J.S.; validation, S.M. and J.-S.S.; investigation, H.K., M.K. and J.S.; data curation, H.K., M.K. and J.S.; writing—original draft preparation, H.K. and M.K.; writing—review and editing, H.K.; supervision, J.-S.S. and J.-Y.Y.; project administration, J.-Y.Y.; funding acquisition, J.-Y.Y. All authors have read and agreed to the published version of the manuscript.

Funding: This research was supported by the Material parts technology development program of Ministry of Trade, Industry and Energy (20003660) and the Characterization platform for advanced materials funded by the Korea Research Institute of Standards and Science (KISS-2022-GP2022-0013-06).

Institutional Review Board Statement: Not applicable.

Informed Consent Statement: Not applicable.

Data Availability Statement: Not applicable.

Conflicts of Interest: The authors declare no conflict of interest.

References

1. Coburn, J.W.; Winters, H.F. Plasma etching—A discussion of mechanisms. *J. Vac. Sci. Technol.* **1979**, *16*, 391–403. [CrossRef]
2. Donnelly, V.M.; Kornblit, A. Plasma etching: Yesterday, today, and tomorrow. *J. Vac. Sci. Technol. A* **2013**, *31*, 050825. [CrossRef]
3. Ito, N.; Moriya, T.; Uesugi, F.; Matsumoto, M.; Liu, S.; Kitayama, Y. Reduction of particle contamination in plasma-etching equipment by dehydration of chamber wall. *Jpn. J. Appl. Phys.* **2008**, *47*, 3630–3634. [CrossRef]
4. Kasashima, Y.; Nabeoka, N.; Motomura, T.; Uesugi, F. Many flaked particles caused by impulsive force of electric field stress and effect of electrostriction stress in mass-production plasma etching equipment. *Jpn. J. Appl. Phys.* **2014**, *53*. [CrossRef]
5. Mun, S.Y.; Shin, K.C.; Lee, S.S.; Kwak, J.S.; Jeong, J.Y.; Jeong, Y.H. Etch defect reduction using SF_6/O_2 plasma cleaning and optimizing etching recipe in photo resist masked gate poly silicon etch process. *Jpn. J. Appl. Phys.* **2005**, *44*. [CrossRef]
6. So, J.; Choi, E.; Kim, J.-T.; Shin, J.-S.; Song, J.-B.; Kim, M.; Chung, C.-W.; Yun, J.-Y. Improvement of plasma resistance of anodic aluminum-oxide film in sulfuric acid containing Cerium(IV) ion. *Coatings* **2020**, *10*, 103. [CrossRef]
7. Kim, M.; Choi, E.; So, J.; Shin, J.-S.; Chung, C.-W.; Maeng, S.-J.; Yun, J.-Y. Improvement of corrosion properties of plasma in an aluminum alloy 6061-T6 by phytic acid anodization temperature. *J. Mater. Res. Technol.* **2020**, *11*, 219–226. [CrossRef]
8. Song, J.-B.; Kim, J.-T.; Oh, S.-G.; Yun, J.-Y. Contamination particles and plasma etching behavior of atmospheric plasma sprayed Y_2O_3 and YF_3 coatings under NF3 plasma. *Coatings* **2019**, *9*, 102. [CrossRef]
9. Deposited, Y.O.; Coatings, Y.F. Contamination particle behavior of aerosol. *Coatings* **2019**, *9*, 310.
10. Kim, M.; Choi, E.; Lee, D.; Seo, J.; Back, T.-S.; So, J.; Yun, J.-Y.; Suh, S.-M. The effect of powder particle size on the corrosion behavior of atmospheric plasma spray-Y_2O_3 coating: Unraveling the corrosion mechanism by fluorine-based plasma. *Appl. Surf. Sci.* **2022**, *606*, 154958. [CrossRef]
11. Ahmed, R.; Faisal, N.; Reuben, R.L.; Paradowska, A.M.; Fitzpatrick, M.; Kitamura, J.; Osawa, S. Neutron diffraction residual strain measurements in alumina coatings deposited via APS and HVOF techniques. *J. Phys. Conf. Ser.* **2010**, *251*, 012051. [CrossRef]
12. Lee, J.-K.; Park, S.-J.; Oh, Y.-S.; Kim, S.; Kim, H.; Lee, S.-M. Fragmentation behavior of Y_2O_3 suspension in axially fed suspension plasma spray. *Surf. Coat. Technol.* **2017**, *309*, 456–461. [CrossRef]
13. Barve, S.; Jagannath; Mithal, N.; Deo, M.; Chand, N.; Bhanage, B.; Gantayet, L.; Patil, D. Microwave ECR plasma CVD of cubic Y_2O_3 coatings and their characterization. *Surf. Coat. Technol.* **2010**, *204*, 3167–3172. [CrossRef]
14. Shin, J.-S.; Kim, M.; Song, J.-B.; Jeong, N.-G.; Kim, J.-T.; Yun, J.-Y. Fluorine Plasma Corrosion Resistance of Anodic Oxide Film Depending on Electrolyte Temperature. *Appl. Sci. Converg. Technol.* **2018**, *27*, 9–13. [CrossRef]
15. Shin, J.-S.; Song, J.-B.; Choi, S.-H.; Kim, J.-T.; Oh, S.-G.; Yun, J.-Y. Plasma Corrosion in Oxalic Acid Anodized Coatings Depending on Tartaric Acid Content. *Appl. Sci. Converg. Technol.* **2016**, *25*, 15–18. [CrossRef]
16. Amin, S.; Panchal, H. A review on thermal spray coating processes. *Int. J. Curr. Trends Eng. Technol.* **2016**, *2*, 556–563.
17. Hwang, Y.-J.; Kim, K.-W.; Lee, H.-Y.; Kwon, S.-C.; Lee, K.A. Effect of spray angle the on microstructure and mechanical properties of Y_2O_3 coating layer manufactured by atmospheric plasma spray process. *J. Korean Powder Met. Inst.* **2021**, *28*, 310–316. [CrossRef]
18. Ma, T.; List, T.; Donnelly, V.M. Comparisons of NF_3 plasma-cleaned Y_2O_3, YOF, and YF_3 chamber coatings during silicon etching in Cl_2 plasmas. *J. Vac. Sci. Technol. A* **2018**, *36*, 031305. [CrossRef]
19. Lee, H.-K.; Lee, S.; Kim, B.-R.; Park, T.-E.; Yun, Y.-H. Microstructure and plasma resistance of Y_2O_3 ceramics. *J. Korean Cryst. Growth Cryst. Technol.* **2014**, *24*, 268–273. [CrossRef]
20. Kwon, H.; Kim, M.; So, J.; Shin, J. A study on plasma corrosion resistance and cleaning process of yttrium-based materials using atmospheric plasma spray coating. *J. Semicond. Disp. Technol.* **2022**, *21*, 74–79.
21. Chen, S.; Sheng, B.; Xu, X.; Fu, S. Wet-cleaning of contaminants on the surface of multilayer dielectric pulse compressor gratings by the piranha solution. In *5th International Symposium on Advanced Optical Manufacturing and Testing Technologies: Advanced Optical Manufacturing Technologies*; SPIE: Dalian, China, 2010; Volume 7655, pp. 489–495.
22. Sirghi, L.; Kylián, O.; Gilliland, D.; Ceccone, G.; Rossi, F. Cleaning and hydrophilization of atomic force microscopy silicon probes. *J. Phys. Chem. B* **2006**, *110*, 25975–25981. [CrossRef] [PubMed]

23. Joyce, R.; Singh, K.; Varghese, S.; Akhtar, J. Effective cleaning process and its influence on surface roughness in anodic bonding for semiconductor device packaging. *Mater. Sci. Semicond. Process.* **2015**, *31*, 84–93. [CrossRef]
24. Lo, Y.-S.; Huefner, N.D.; Chan, W.S.; Dryden, P.; Hagenhoff, B.; Beebe, T.P. Organic and inorganic contamination on commercial afm cantilevers. *Langmuir* **1999**, *15*, 6522–6526. [CrossRef]